sustainability

MDPI

Review

A Review on the Impact of High-Temperature Treatment on the Physico-Mechanical, Dynamic, and Thermal Properties of Granite

Soumen Paul [1], Somnath Chattopadhyaya [2], A. K. Raina [3], Shubham Sharma [4,5,*], Changhe Li [5], Yanbin Zhang [5], Amit Kumar [6] and Elsayed Tag-Eldin [7,*]

[1] Department of Mechanical Engineering, Bankura Unnayani Institute of Engineering, Bankura 722146, West Bengal, India
[2] Department of Mechanical Engineering, Indian Institute Technology (Indian School of Mines), Dhanbad 826004, Jharkhand, India
[3] CSIR-Central Institute of Mining and Fuel Research, Nagpur Research Center (Mining Technology), 17/C Telangkhedi Area, Civil Lines, Nagpur 440001, Maharashtra, India
[4] Mechanical Engineering Department, University Center for Research & Development, Chandigarh University, Mohali 140413, Punjab, India
[5] School of Mechanical and Automotive Engineering, Qingdao University of Technology, Qingdao 266520, China
[6] Department of Mechanical Engineering, Institute of Engineering & Technology, GLA University, Mathura 281406, Uttar Pradesh, India
[7] Faculty of Engineering and Technology, Future University in Egypt, New Cairo 11835, Egypt
* Correspondence: shubham543sharma@gmail.com or shubhamsharmacsirclri@gmail.com (S.S.); elsayed.tageldin@fue.edu.eg (E.T.-E.)

check for updates

Citation: Paul, S.; Chattopadhyaya, S.; Raina, A.K.; Sharma, S.; Li, C.; Zhang, Y.; Kumar, A.; Tag-Eldin, E. A Review on the Impact of High-Temperature Treatment on the Physico-Mechanical, Dynamic, and Thermal Properties of Granite. *Sustainability* **2022**, *14*, 14839. https://doi.org/10.3390/su142214839

Academic Editors: Chaolin Zhang and Jianjun Ma

Received: 7 September 2022
Accepted: 6 November 2022
Published: 10 November 2022

Abstract: Temperature changes have significant effects on rock properties. The changes in properties vary for different rocks with different temperature ranges. Granite is an igneous type of rock that is common in India and is frequently used for construction and domestic purposes. Granite is mainly composed of quartz and feldspar and shows a considerable response to temperature changes and is the subject of this paper. A comprehensive review of the published literature has been conducted in this paper. Comparison of the findings of such works in terms of the impact of temperature changes on basic mechanical, physical, and thermal properties of granite, viz. thermal damage, density, p-wave velocity, compressive strength, peak stress, peak strain, and Young's modulus from room temperature to 1000 °C has been conducted. The published data of different researchers have been utilized for such comparison. The study revealed that there is a significant departure in response to the rock recorded by various researchers, which may be due to the constitution of the rocks analyzed or experimental procedures. This points to the standardization of such tests. The main reason for changes in the properties of granite has also been discussed. Consequently, the findings of this state-of-the-art demonstrate that the heating effects of granite on its physical and mechanical properties become increasingly pronounced with increasing pick temperatures. The purpose of this article is to provide readers with an extremely well-structured, seamless environment that facilitates a critical assessment of granite in order to determine its thermal profile.

Keywords: granite; temperature changes; thermal damages; physico-mechanical properties; dynamic properties

1. Introduction

The role of temperature change of rocks in the mechanical weathering of rocks over time is a well-established concept in geology [1–3]. The temperature changes have a profound effect on the physical, mechanical, dynamic, and thermal properties of the rocks [4–7]. The thermal change may happen in various ways. It may be heating and

followed by slow cooling or fast cooling/quenching method or cyclic freeze–thaw method. A host of the literature is available on the thermal effects of rocks at different low- to high-temperature limits [8–10]. A comparison of heat treatment of granite by different authors is compiled in Table 1. At high temperatures, rocks increase the resistance several times with a reduction of plasticity [11–13]. In recent decades, the temperature effects on rocks have become popular due to the development of technologies and underground mining activities [14–16]. At high temperatures, the structural changes lead to the effects on mechanical properties and physical properties, which are the basic phenomenon of the materials. The critical assessment of the thermal profile while drilling granite material is of utmost importance. The elevated temperature will deform the drilling tool to a great extent [17–19]. The elevated temperature generated through drilling activities challenges the hot hardness and hot toughness of the drilling tool material. In order to make a realistic and pragmatic strategy [20,21]. The understanding of heat generation during drilling is very much crucial. However, there is a significant departure in the findings of such research.

Table 1. Comparison of heat treatment of granite by various authors.

Year	Ref. [No.]	Factors Treated	Rock		Petrological Character	Temperature Variation	Method Used	Objective	Comments
			Name	Location					
1985	[22]	Heat treated	Stripa granite	Central Sweden	Quartz 35%, Plagioclase 35%, Microcline 24%, Muscovite 2%, Chlorite 3%, Accessories 1%.	100 °C to 600 °C	Optical microscopy, SEM, and differential strain analysis (DSA)	Microcrack density and fractural mechanical properties	-
2007	[16]	Heat treated	Westerly granite	Brazil	-	Room temperature to 850 °C	Mode I Tensile Test.	Fractural toughness and wave velocities	Rock behavior UP to 850 °C temperatures.
2007	[8]	High-temperature treatment	Westerly granite	Brazil	Plagioclase 46%, Quartz 42%, Feldspar 8%, Mica 4%.	25 °C to 850 °C	Tensile Test Heat treatment	Crack density and wave velocity of Westerly granite	
2008	[9]	Thermal damages	Beishan Granite	France	46% plagioclase, 8% K-feldspar, 42% quartz, and 4% mica.	Room temperature to 600 °C	Gas permeability, velocity, and attenuation of ultrasonic waves	Porosity, permeability, ultrasonic velocity measurement	Rock behavior at each stage of heat treatment.
2014	[18]	Heat treated	Beishan granite	China	49.42 to 51.26% K-feldspar, 20.37 to 21.46% quartz, 18.74 to 20.89% plagioclase, and 8.23 to 10.36% biotite.		Compression test	Permeability variation and microcrack	-
2015	[6]	Mechanical behavior on high-temperature treatment	Australian Strathbogie granite	Australia	-	Room temperature to 800 °C	Acoustic emission, electron microscopic scanning.	Geothermal energy	Changes observed between 600 °C to 800 °C
2016	[4]	Temperature changes	Strainbrust granite	China	-	30 °C to 700 °C	Acoustic emission.	Triaxial loading	Changes observed between 300 °C to 700 °C
2017	[5]	High-temperature treatment	Granite	China	11.12% quartz, 59.85% feldspar, 21.56% biotite, 6% amphibole, 1.01% chlorite, and 0.46% dolomite.	25 °C to 800 °C	Uniaxial Compressive test and acoustic emission test	Experimental investigation	Ductile deformation between 700 °C to 800 °C

Table 1. *Cont.*

Year	Ref. [No.]	Factors Treated	Rock		Petrological Character	Temperature Variation	Method Used	Objective	Comments
			Name	Location					
2017	[12]	Physical, Mechanical properties of granite	Jalore granite	India	-	25 °C to 600 °C	Scanning electron microscope (SEM) analyses	High-temperature treatment	Thermal cracking of brittle rock
2019	[1]	Thermal treatment of granite	-	-	-	Room temperature to 500 °C	Non-destructive test and destructive test.	Slow cooling and rapid cooling	Changes observed in different temperature ranges
2020	[23]	Physical and Mechanical properties		China		200 °C to 800 °C	Liquid Nitrogen cooling treatment	Different rate of cooling	Observation of crack generation.

This paper has thus been formulated to investigate such published data and present a critical review of the methods and observations found in the published domain while focusing on granite, as the same is widely used in India in domestic and industrial structures. Moreover, granite has been used hugely due to its long lifetime, heat resistance, minimal chemical reactivity, and high hardness that prevents scratches [22,24,25]. The study will help to evaluate the methods and aid in defining new standards for such testing.

2. Influence of Temperature on Physical Properties

2.1. Stress–Strain

An increase in temperature results in the sudden fracturing of the rock surfaces. Su et al. [4], while studying strain burst of rocks, concluded that the kinetic energy increases with an increase in temperature up to 300 °C but decreases sharply at temperatures between 300 °C to 700 °C [26–28]. Sheng-Qi et al. [5] observed that Poisson's ratio first decreases up to 600 °C then increases rapidly up to a temperature of 800 °C with ductile failure due to axial stress and the development of tensile crack [29–31]. In the study on fine-grained granite [6], the authors observed that the stress threshold decreases with increased temperature and the cracks propagate in stable conditions as evidenced by acoustic emission signatures. Similar observations were recorded in the Australian Strathbogie Granite [7] with thermal shock. Effects of tensile stress and thermal crack/microstructure distribution on heat-treated five sets of samples of the Westerly Granite were reported [8,32,33]. Chaki et al. [9] presented a study on the temperature effects of granite up to 600 °C, observed the rock behavior in different stages, and presented a consistency between mechanical, transport, and physical properties [34–36].

The temperature changes in granite affect the peak stress and decrease due to an increase in temperature. In the temperature range between 25 °C to 100 °C, the peak stress behaves almost linearly, and this non-linearity depends on the geometry and initial density of cracks [37–39]. The free water evaporates with an increase in temperature, and the density of the rock decreases with a decrease in peak stress [40–42]. This introduces the cracks; pores with an increase in the axial pressure further enhance the crack propagation. The relationship between peak stress and temperature is represented by a quadratic function [2,43,44].

$$\sigma = 221.92 - 0.82T + 1.75 \times 10^{-3}T^2 \quad (1)$$

where σ denotes the peak stress, and T represents the temperature.

Due to changes in temperature from room temperature to 300 °C, the peak stress increases slightly, but after 300 °C, it decreases [4,45,46] with an overall 80% decrease from room temperature to 1000 °C [6,47,48] (Table 2, Figure 1). The rate of change of peak stress reduces after 400 °C [10,49,50]. The increase in temperature affects the kinetic energy of the particles, and thus, the energy release rate is related to the stress of the material [23,51].

Table 2. Stress (MPa) of Granite.

Peak Stress															
Ref No.	Granite Type	Temperature (°C)													
		25	30	35	50	100	200	300	400	500	600	700	800	900	1000
[2]		206.4			183.3	150.3	136.5	131.3							
[4]			255.9			253.2	250	253.3	245.9	243.7	222.7	199.9			
[6]		85.54					76.19		71.77		31.7		18.8		13.41
[15]	Jalore	66.72					68.01	69.1	52.9	41.45	32.71				
[23]	General	115.39					108.54		94.048		49.87		38.07		
[52]		252.75					234.44	230.37	223.7	172.61	112.71				

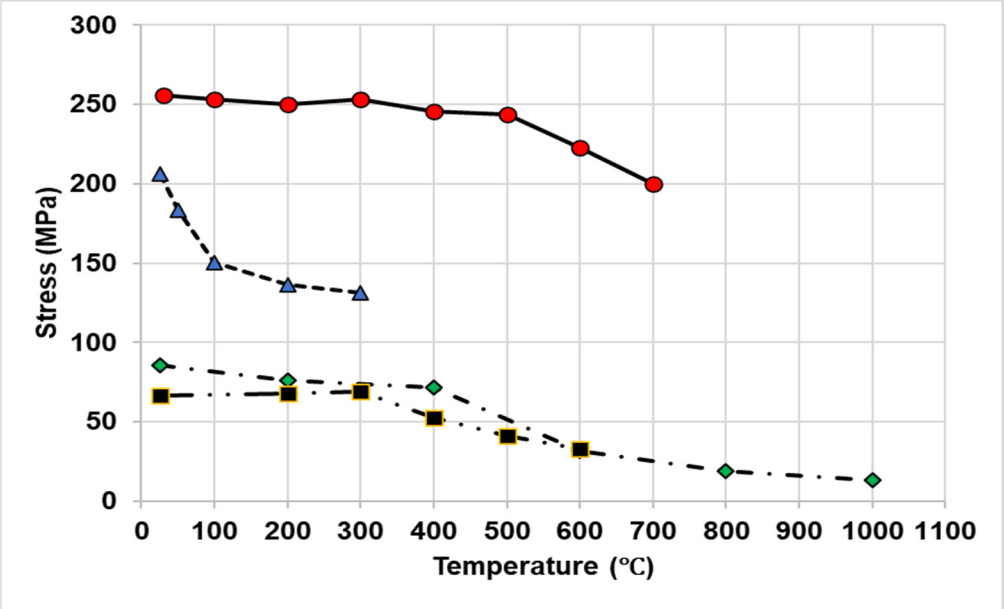

Figure 1. Stress vs. temperature. Different symbol lines represent data from refs. [2,4,6,15].

Strain is the measure of deformation or displacement of body particles of a material. Rock is a heterogeneous material, and the nature of deformation is distinct from metals. The stability of rocks is measured with the help of the post-peak strain. Peak strain deformation is an important strategy to evaluate in the geo-mechanical field [11]. Due to temperature effects, the internal structure of rocks is in stretchable condition with the development of new cracks. The internal strain developed within rocks varies with temperature. The peak strain increases with an increase in temperature initially, and after 300 °C, the rate slows down. A quadratic equation represents the change in peak strain under rising temperature as:

$$\epsilon = 4.1 \times 10^{-3} + 4.96 \times 10^{-6} T - 9.46 \times 10^{-9} T^2 \quad (2)$$

where ϵ denotes the strain, and T is the temperature of the material.

From the experiments, it was found that the peak strain varies slightly from the temperature range between 30 °C to 300 °C. From the temperature range between 300 °C to 700 °C, the peak stain increases linearly [4]. The peak strain between the temperature range of 700 °C to 1000 °C increases three times more than the initial condition [6]. The peak strain of granite initially increases around 7% from room temperature to 100 °C, nearly 4% up to 200 °C and remains near constant after 300 °C. At the initial stage the strain is non-linear due to the opening of micro cracks, and their density is non-linear due to an increase in temperature.

The range of elastic deformation is obtained by the ratio of radial strain to axial strain. The peak axial strain is near constant up to 300 °C temperature, then increase by 18% up to

400 °C. It was further observed that the peak strain increases up to three times from room temperature to 1000 °C [5]. Table 3 and Figure 2 indicate the nature of strain changes with temperature changes seen in the published literature.

Table 3. Strain of Granite.

Peak Strain															
Ref No.	Granite Type	Temperature (°C)													
		25	30	35	50	100	200	300	400	500	600	700	800	900	1000
[2]		0.00424			0.00427	0.00452	0.004722	0.004758							
[4]			0.107			0.108	0.111	0.102	0.112	0.11	0.123	0.149			
[5]		0.215					0.259	0.248	0.284	0.264	0.372	0.542	0.584		
[6]		0.01721					0.01666		0.0187		0.0298		0.0402		0.0527
[7]	Strathbogie	0.027				0.026	0.032		0.03		0.026		0.04	0.058	0.057
[52]		1.43					0.949	0.916	0.983	1.209	1.244				

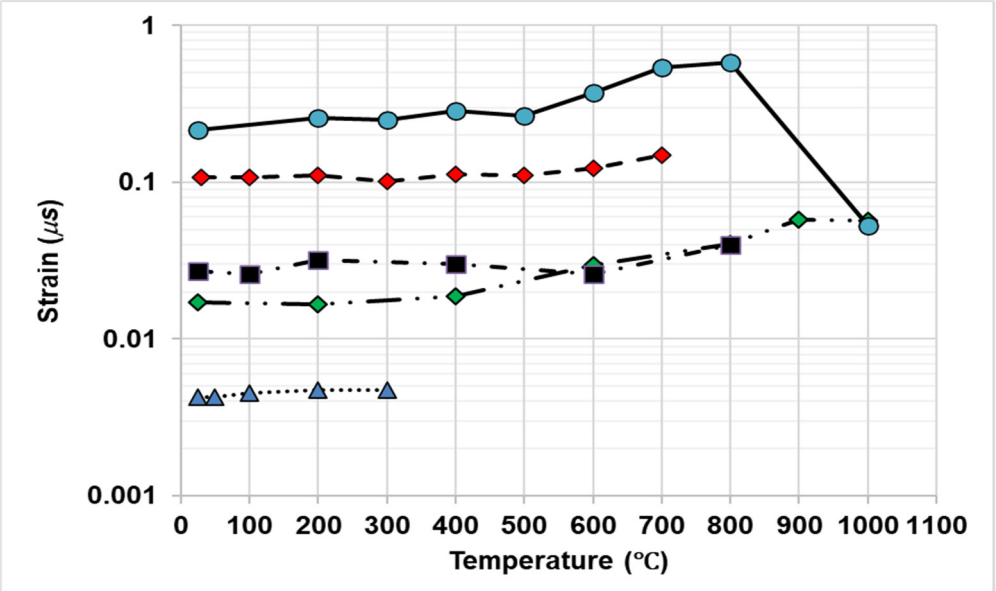

Figure 2. Strain vs. temperature. Different symbol lines represent data from refs. [2,4–7].

2.2. Density

Density is the intrinsic property of rocks. The average density of granite lies between 2650 to 2750 kg/m^3. The density of rocks depends on three basic factors, i.e., temperature, pressure, and composition. During heating, the dry, tough outer part expands and leads to a decrease in density. It was observed that the density of heat-treated rocks decreased gradually [1]. The impact on the dense bonding of molecules after high-temperature heating may also decrease the density. The density also depends on the basis of thermal damage and the quality of the materials. The rate of losing mass shows an increasing trend with an increase in temperature. So, the mass of granite decreases after high-temperature treatment. Such a rate is lesser in the case of a rapid quenching process [1] than in slow cooling. The volume of granite also increases with an increase in temperature. The thermal expansion of axial and lateral strain causes the micro-cracking of granite minerals. The computed tomography (CT) number is generally a function of the density and chemical composition of the material [5]. Dehydration of molecules and tight bonding may cause a decrease in the density of granite [12]. From Table 4, it can be observed that the density decreases with an increase in temperature. The density indicates a moderate decrease, but the rate of decrease is not so high. Figure 3 shows the density changes of granite on heat treatment along with the variation in results obtained by various authors cited above.

Table 4. Density (kg/m^3) of Granite.

Density															
Ref No.	Granite Type	Temperature (°C)													
		25	30	35	50	100	200	300	400	500	600	700	800	900	1000
[1]		2637.6				2637.3	2628.3	2624.6	2616.33	2608.6	2577.6				
[2]		2622.9			2616.83	2604.19	2583.33	2556.87							
[5]		2643					2645	2650	2644	2640	2650	2647	2638		
[15]	Jalore	2609.16					2597.4	2550.78	2532.57	2469.88	2407.93				
[23]	General	2644.4					2648.65		2636.11		2649.65		2652.84		
[52]		2591					2599	2598	2592	2598	2594				

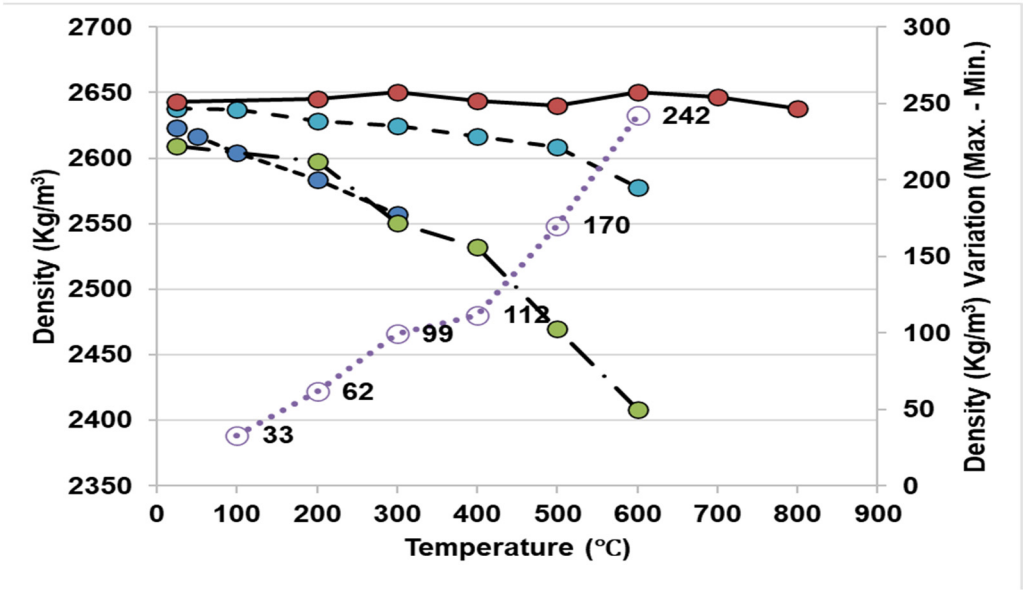

Figure 3. Density vs. temperature. Different symbol lines represent data from refs. [1,2,5,15].

Figure 3 (see Table 4) illustrates an interesting fact: despite an initial average density of 2628 kg/m^3 and a standard deviation of a mere 13 kg/m^3, there is increasing variation ranging from 33 to 242 kg/m^3 in density after heat treatment at 600 °C. This has a significant connotation in terms of methods deployed for such tests.

2.3. Porosity

Granite is generally non-porous, but some in situ spaces may result in porosity. Porosity is defined as the ratio of a volume of void space with in a rock to the total bulk volume of the rock. It can be expressed as a general equation as follows.

$$\varnothing = \frac{V_{pores}}{V_{rock}} \quad (3)$$

where $\varnothing$ is the porosity of rocks, V_{pores} is the volume of void space, and V_{rock} is the total bulk volume of rock.

Yang et al. [5] investigated the physical behavior of granite from room temperature to 800 °C. It was observed that from 25 °C to 300 °C, the porosity decreases 0.828% to 0.685%. Then, porosity increases from 0.685% to 3.460% up to a temperature of 800 °C due to the rapid formation of micro-cracks. During the opening of micro-cracks and reproduction of new cracks between temperatures from 100 °C to 500 °C, some structural changes are induced, and as a result, the porosity increases. The increasing rate is noticeable after 500 °C with a large increase in cracks [9]. Moreover, a high temperature results in the

evaporation of water molecules from the minerals [12]. Generally, the porosity of granite ranges from 0.2% to 0.8% at normal temperatures. However, it increases up to 2.85% at 600 °C [13]. Vagnon et al. [14] established an exponential relationship between porosity and temperature from experimental data and pointed out that the porosity increases up to 3% at 600 °C. The crack propagation and the rate of increase in porosity are effective at 500 °C to 600 °C [15,16]. The heterogeneity of minerals generates new cracks due to thermal expansion at high temperatures and hence an increase in porosity [17]. Guangsheng Du et al. have analyzed the temperature generation and the effect of the temperature on rock microstructure changes which are basically granite rocks, as indicated by an analysis of the micro-inhomogeneity. Denature of crystal takes place when the temperature rises above 400 °C [53]. Table 5 and Figure 4 indicate the change of porosity with an increase in temperature.

Table 5. Porosity (%) of Granite.

Porosity															
Ref No.	Granite Type	Temperature (°C)													
		25	30	35	50	100	200	300	400	500	600	700	800	900	1000
[9]						0.63%	0.82%	1.08%	1.26%	1.43%	2.98%	5.35%			
[16]											2.10%		7.30%		10.60%
[16]											0.80%		5.90%		7.50%
[24]		0.87%			0.75%	0.74%	1.01%	1.41%		1.33%			2.57%		
[23]		1.63%					3.16%		3.86%		9.67%		14.02%		

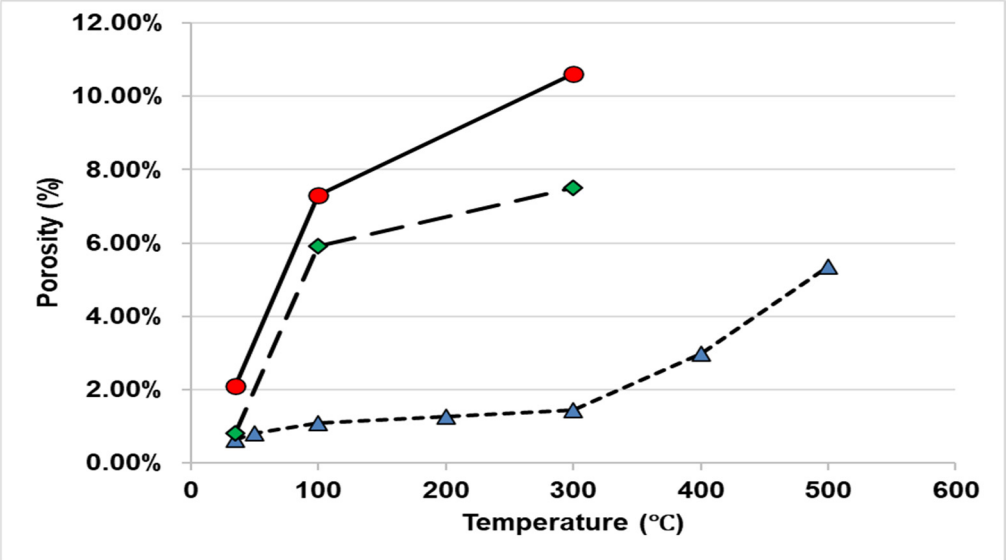

Figure 4. Porosity vs. temperature. Different symbol lines represent data from refs. [9,16].

2.4. Permeability

The permeability of rocks depends on void space, grain size, and the cementation of mineral constituents. However, if the rock pores are isolated from one another, then the rock would be impermeable. A triaxial compression experiment was conducted on Beishan granite [18] to measure the permeability changes in crack effected region. A permeability changes model was established and was presented with the help of a numerical simulation technique. The heat treatment process on the Beishan Granite up to 800 °C [19] concluded that the cracks developed due to the phase transformation of quartz and hence changed in permeability under unconfined conditions. Moore et al. [20] examined the rate of decrease of permeability from 300 °C to 500 °C and observed that after 400 °C decreasing rate of

permeability is high due to greater reactivity of the material. The permeability of the rapidly cooled sample shows increases in porosity than the slowly cooled samples [21] and is directly dependent on crack formation.

Thermal effects on Jalore granite to examine the mechanical and physical properties were performed up to 600 °C [12], and the results were compared to granites of other countries. The authors [12] also observed the changes in the water content and mineral in the granite specimen with the temperature. Isaka et al. [13] analyzed the micro-structure distribution and the basic difference of crack propagation of slow cooling and rapid cooling of the Harcourt Granite up to 1000 °C. The pore connectivity model and shock induced during cooling were also observed. An experiment on the Stripa Granite up to a temperature range of 600 °C [22], with the help of an optical microscope, pointed to the distribution of elastic and fractural properties of rocks. Homend and R. Houpert [15] predicted the thermal crack propagation and estimation of crack porosity under tensile as well as compressive loading of a granite sample at a heating range between 20 °C to 600 °C. Hewze [24] presented a review article on the high-temperature treatment of granite and an analysis of the different thermo-mechanical properties of rocks. Liu and Xu [25] conducted a study on the Qinling Biotite granite under high-temperature treatment to assess the rock stability and protection for constructional progress at underground technology. Nasseri et al. [16] presented a study on the Westerly Granite for analysis of crack density and porosity with an increase in temperature, and they predicted a relation between the fractural length and crack density of the sample. Xu et al. [17] conducted an experiment on granite up to 1200 °C to predict the tensile fractural stress and microstructure analysis to determine the chemical characteristic of rocks. Yin et al. [26] analyzed the failure made of granite under different temperature limits, especially the splitting failure and shear failure. Chen et al. [27] presented a study on heat treatment of granite up to 800 °C to observe the microstructural mineral changes in granite with the help of scanning electron microscopy while analyzing such rocks for different mechanical properties changes under the temperature. Wu et al. [28] analyzed the effect of nitrogen cooling on heat-treated granite specimens and observed the mechanical and physical properties changes in medium- and fine-grained granite. Yang et al. [29] conducted a simulation method of failure of granite material containing preexisting holes under different temperatures to observe the meso-mechanics of granite material and distribution of crack propagation. Zhao et al. [30] presented a study on the thermally treated Beishan Granite up to 400 °C for rough fracture and micro-crack generation. This study also highlighted the shear fracture property changes with an increase in temperature. Zuo et al. [31] carried out an experiment on Beishan Granite under high-temperature treatment with the help of a Scanning Electron Microscope. They observed that the direction of micro-crack generation depends on the distribution of the mineral grains. They also determine the elastic modulus and stress intensity factors. Dong Zhu et al. [54] conducted a Brazilian splitting test on granite material to investigate the effect of heating and cooling on the mechanical properties of granite. They also observed the plasticity increases with an increase in temperature. Xiangxi Meng et al. [55] have discussed the thermal cracking and permeability changes under the uniaxial compressive test of granite at a temperature of 100 °C to 650 °C. They have observed that the permeability of granite increases above the critical temperature.

3. Influence of Temperature on Mechanical Properties

Mechanical properties like Young's modulus, Poison's ratio, tensile strength, compressive strength, and p-wave velocity record changes with an increase in temperature. A few publications addressing such changes by various authors up to 1000 °C are reviewed here.

3.1. Young's Modulus of Elasticity

Young's modulus is a measure of the stiffness of a material under tension and compression. Basically, it is a relation between stress and strain of a material. Young's modulus is a measure of the characteristic of a material and is used in geo-mechanical engineering

design [32]. Young's modulus generally decreases due to an increase in temperature. The decreasing rate is more enhanced in the rapid cooling method than in the slow cooling method [1]. The dynamic damages basically depend on the elastic modulus and wave velocity of the material. The elastic modulus is classified into three basic categories, i.e., initial elastic modulus, tangent elastic modulus, and secant elastic modulus [2]. The slope of the linear elastic stage is represented by this equation:

$$E = \frac{\sigma_2 - \sigma_1}{\varepsilon_2 - \varepsilon_1} \tag{4}$$

where E is elastic modulus, σ_1 and σ_2 are initial and terminated stress, respectively, ε_1 and ε_2 are initial and terminated strains of the material tested.

The relationship between elastic modulus and wave velocity can be represented by the following equation [2]:

$$E = \frac{(1+\mu)(1-2\mu)}{(1-\mu)}\rho v^2 \tag{5}$$

where E and μ represent the elastic modulus and Poisson's ratio, respectively. The ρ and v are the density and longitudinal wave velocity of the material.

The dynamic and static elastic modulus decrease with an increase in temperature. Young's modulus of granite after high-temperature treatment shows a decreasing trend. The rate of decrease of static modulus is higher than the dynamic modulus for the same temperature variation rate [5]. The elastic modulus decreases rapidly after 400 °C to 800 °C, and the rate of decrease is around 10% than the room temperature [6]. It was observed that the decreasing rate is more extreme in the case of rapid quenching than in slow cooling. The decreasing rate of '*E*' during rapid quenching and slow cooling is about 60% and 50% up to 600 °C temperature, respectively [1]. The rate of decrease in Young's modulus creates thermal cracks, which decrease the strength of the materials [33,34]. The change of elastic modulus usually effects on elastic stages of the stress–strain curve, and it causes dynamic damage to the material [2].

In case of strain burst in the granite sample, Young's modulus reduces with an increase in temperature. The strain distribution is due to changes in Young's modulus and the yield point [4]. With an increase of temperature up to 800 °C, the stress–strain curve of the granite becomes non-linear, and the material reaches a yielding point. If the temperature limit is high, the materials deform slowly and with thermally deformation cracks that affect the fracture propagation [5]. If the temperature increases up to 1000 °C, the elastic modulus decreases by 20% of the normal value [6]. In the case of the Strath Bogie Granite, the rate of decrease of Young's modulus is about 15% between temperatures 600 °C to 800 °C [7]. The constant slow-temperature heating and varying temperature rapid-heating effects on the mechanical behavior of granite, and slow cooling prevents the thermal shock after heating along with decreasing Young's modulus [9]. The elastic modulus tends to steady state up to a temperature of 200 °C due to less dependency on the elastic property of granite. Then, between 300 °C to 800 °C decreases gradually with an increase in temperature [10]. After 400 °C, it was found that the elastic modulus is greater in the case of fine-grain granite than the medium-grain and coarse-grain granite. The crack density increases, and the thermal crack development is the main reason for such diverse nature of elastic modulus during heating [20]. Table 6 represent the different values of Young's modulus, and Figure 5 highlights the statistical observation of Young's modulus changes of different temperature in the published literature.

A substantial variation in E can be observed in Figure 5 and needs to be investigated further. In the absence of complete mineralogical and petrological data in cited publications, it is difficult to ascertain the cause of such variation in E.

Table 6. Young's Modulus of Granite.

Young's Modulus.															
Ref No.	Granite Type	Temperature (°C)													
		25	30	35	50	100	200	300	400	500	600	700	800	900	1000
[1]		12.81				12.96	11.92	11.25	11.04	10.78	6.45				
[2]		44.04			41.86	35.19	28.21	26.78							
[4]			32.8		30.2	31.1	30	28.7	25.6	24.6	21				
[5]		37.35					36.26	40.73	32.45	25.18	16.88	4.842	2.068		
[6]		14.78					14.48		14.45		7.39		1.5		0.81
[7]	Australian Strathbogie	8.97				8.28	8.48		7.94		5.77		3.72		1.34
[9]	Beishan					22.29	22.64	22.74	21.52	20.5	17.17	12.41			
[10]	Australian	17.13				16.51	15.97	14.5	12.47	10.13	6.89	2.9	0.91		
[13]	Fine-grained	8.97					13.96		14.06		11.91		10.81		
[13]	Medium-grained	8.57					11.76		13.49		9.63		1.99		
[13]	Coarse-grained	8.87					14.33		14.56		8.11		3.51		
[23]	General	32.60					31.78		25.79		10.59		6.96		
[52]		24.35					22.74	22.69	21.62	20.26	13.17				

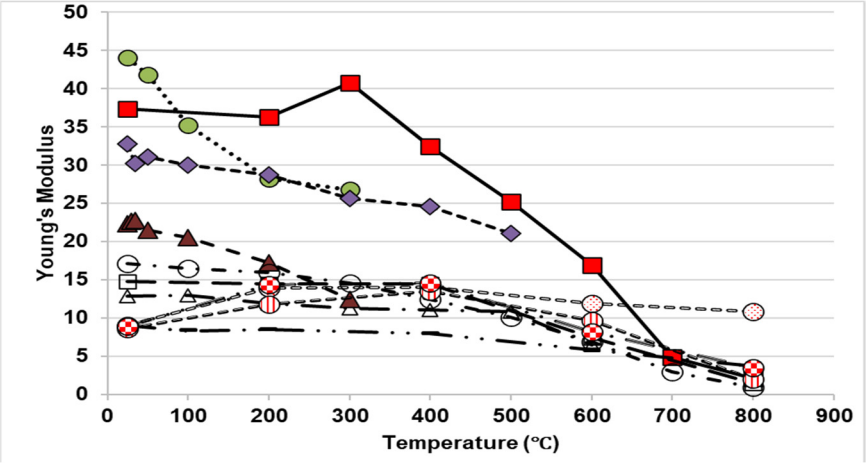

Figure 5. Young's Modulus vs. temperature. Different symbol lines represent data from refs. [1,2,4–7,9,10,13].

3.2. Poisson's Ratio

Poisson's ratio is one of the most important deformation mechanical properties indicating the brittle–ductile transition characteristic of a rock. Poisson's ratio is the ratio of the transverse contraction strain to the longitudinal extension strain. It was observed that up to 500 °C, the Poisson's ratio decreases by 25% for the slow cooling process but in the case of the rapid cooling process, the reduction rate of Poisson's ratio is 20% up to 300 °C [10]. However, up to 800 °C, the Poisson's ratio increases by 38% for slow cooling and 50% for the rapid cooling process. The reduction of Poisson's ratio is due to micro-crack generation and an increase in transverse strain.

The Poisson's ratio is related to the ratio of p-wave velocity and s-wave velocity. The ratio decreases as the temperature increases [14]. Aim et al. [22] observed the Poisson's ratio changes in Stripa Granite up to 600 °C in two unconfined stress conditions. Homond-Etienne and Houpert [15] observed a negative Poisson's ratio of granite in compression as well as in tensile stress conditions up to 600 °C. The abnormality sign of lateral strain leads negative Poisson's ratio, which is theoretically considered for isotropic material. Yang et al. [5] tested the ratio in granite up to 800 °C. They observed that the static Poisson's ratio decreases from 0.127 to 0.038 up to 600 °C and then increases rapidly from 0.038 to

0.367 up to 800 °C. However, the dynamic Poisson's ratio does not depend on the temperature. Wu et al. [28] showed that the Poisson's ratio does not show a noticeable effect on cyclic heating and cooling due to rock heterogeneity. Table 7 and Figure 6 show the change in Poisson's ratio with temperature.

Table 7. Poisson's Ratio of Granite.

Poison's Ratio															
Ref No.	**Granite Type**	**Temperature (°C)**													
		25	**30**	**35**	**50**	**100**	**200**	**300**	**400**	**500**	**600**	**700**	**800**	**900**	**1000**
[10]	Slow cooling					0.22	0.21	0.19	0.18	0.18	0.21	0.32	0.33		
[10]	Rapid cooling					0.21	0.2	0.19	0.25	0.25	0.21	0.35	0.36		
[5]	Static						0.098	0.109	0.095	0.041	0.038	0.0244	0.367		
[5]	Dynamic						0.461	0.461	0.454	0.454	0.449	0.462	0.452		

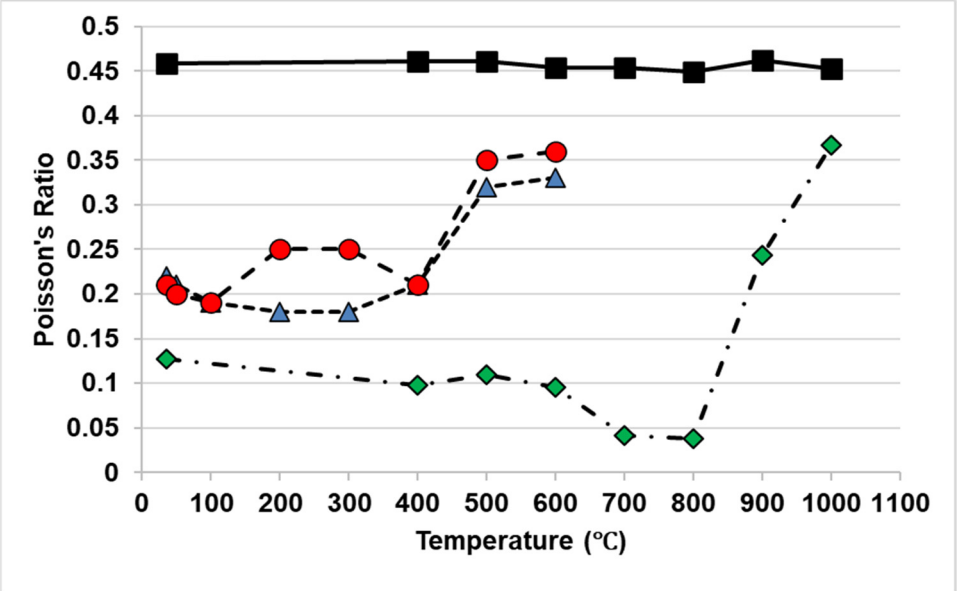

Figure 6. Poisson's Ratio vs. temperature. Different symbol lines represent data from refs. [5,10].

3.3. Compressive Strength

The compressive strength of a material is the capacity to withstand the load under compression. The compressive strength is basically performed for stress–strain analysis of a material under different loading conditions. Compressive strength [35] determined at different temperatures revealed that it decreases with an increase in temperature [1,35]. The tests were performed under different heat treatment conditions, i.e., under slow cooling–heating or rapid heating–cooling and also quenching in a different medium. In the case of slow cooling, it was observed that the compressive strength reduces by about 5%, but strength reduces when heating the sample beyond 600 °C.

From the experimental results, it was found that the compressive strength first increases slightly up to 300 °C and then decreases gradually up to 800 °C [5]. As the rocks are heterogeneous materials, the strength distribution is unequal in different positions, and the stress concentration affects the formation of cracks. The expansion of the thermally affected rock matrix reduces the distance of minerals, resulting in the enhancement of the bonding strength. So, firstly, the overall strength increases [36,37]. Further, the increase in temperature results in the weakening of grain boundaries, permanent damage to the rock due to the formation of cracks, and a decrease in compressive strength. The rapid cooling method significantly reduces the compressive strength than the slow cooling method due to the

thermal shock [10]. Jinhui Xu et al. describe the typical dynamic mechanical characteristic of granite material under strain and temperature. They have discussed that the dynamic compressive strength manifests and increments when the rise of temperature is from 50 °C to about 100 °C. Dynamic compressive strength after that point becomes reduced with higher temperature. However, the elastic modulus becomes more sensitive toward the change in temperature in comparison to the strength rate. The damages related to thermal behavior appreciably decrease at a lower temperature. They recommended that 110 °C is a critical temperature that inflicts alteration in thermomechanical properties and has a relationship with the dynamic strength of granite samples [56]. Sheng-Qi Yang et al. [57] experimented on granite up to 800 °C temperature. The axial compressive test was conducted, and thermal damages, strength, and deformation were measured. Kai Chen et al. [58] have conducted the uniaxial compressive test of heat-treated granite, and the Weibull distribution damage law demonstrates the analysis of the damage behavior of granite. Table 8 provides the values of compressive strengths vs. temperature as published by various researchers. Figure 7 is a plot of such data of compressive strength temperature effects.

Table 8. Tensile Strength (MPa) of Granite.

Peak Stress															
Ref No.	**Granite Type**	**Temperature (°C)**													
		25	**30**	**35**	**50**	**100**	**200**	**300**	**400**	**500**	**600**	**700**	**800**	**900**	**1000**
[1]	Slow cooling	7.93				7.623	7.39	6.84	6.46	4.06	2.17				
[1]	Rapid cooling					6.62	6.44	5.15	4.92	3.5	1.753				
[15]	Jalore	8.87					9.91	8.5	3.88	2.65	1.35				

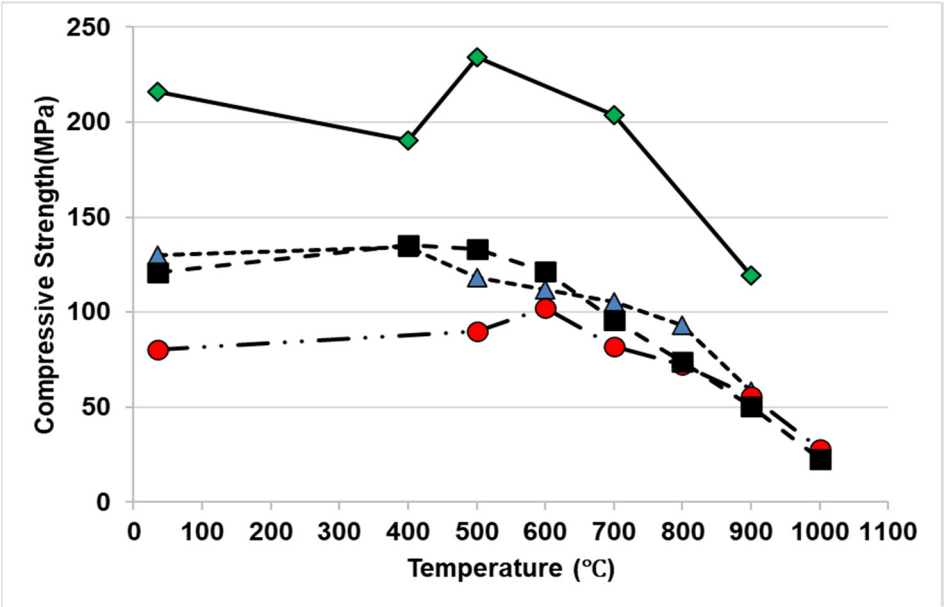

Figure 7. Compressive Strength vs. temperature. Different symbol lines represent data from refs. [1,5,7,10].

3.4. Tensile Strength

Tensile strength of granite after thermal treatment for both slow cooling and rapid quenching show decreasing trends (Figure 8 and Table 9). In the slow cooling process, the reduction rate of tensile strength is 73% up to 600 °C and about 78% for the rapid cooling process. After 400 °C, the rate of decrease of tensile strength changes sharply [1]. Gautam et al. [12] observed that the tensile strength of Jalore Granite increased gradually up to 300 °C due to the expansion of rock molecules and compact specimen, but beyond

this temperature, the tensile strength decreased sharply up to 600 °C. The sharp decrease beyond 300 °C is ascribed to the loss of water molecules and minerals from the material, the expansion coefficient of minerals, and the distribution of thermal stress. In the case of the Stripa Granite, tensile strength first increased slightly up to 100 °C then decreased up to 600 °C due to the increase in the microstructure of the material [22]. The tensile strength of the Senones Granite decreased more rapidly than the Remiremont Granite up to 600 °C due to an increase in the density of micro-crack [15]. The tensile strength of Biotite Granite decreased up to 1000 °C from 25 °C with decreasing rate of 35% [25]. The tensile strength of granite decreased by about 20% when it was in cyclic heating to 600 °C and subsequent quenching in liquid nitrogen [28]. R. Tomas et al. [59] conducted an experiment on 46 cubic granite samples, heating the temperature from 105 °C to 700 °C and cooling the specimen in different conditions. They have observed that the tensile stress is different between the two adjacent particles and improved the hardening effect of granite. The elastic modulus improved due to the hardening effect when the temperature was below 500 °C. Timo Saksala [60] approaches a 3D numerical prediction model to predict the effect of the tensile strength of granite. The sample is heated up to Curie point (near 527 °C), and then the sample is cooled down with air. The simulation results are validated to predict the tensile strength analysis and induced thermal crack propagation.

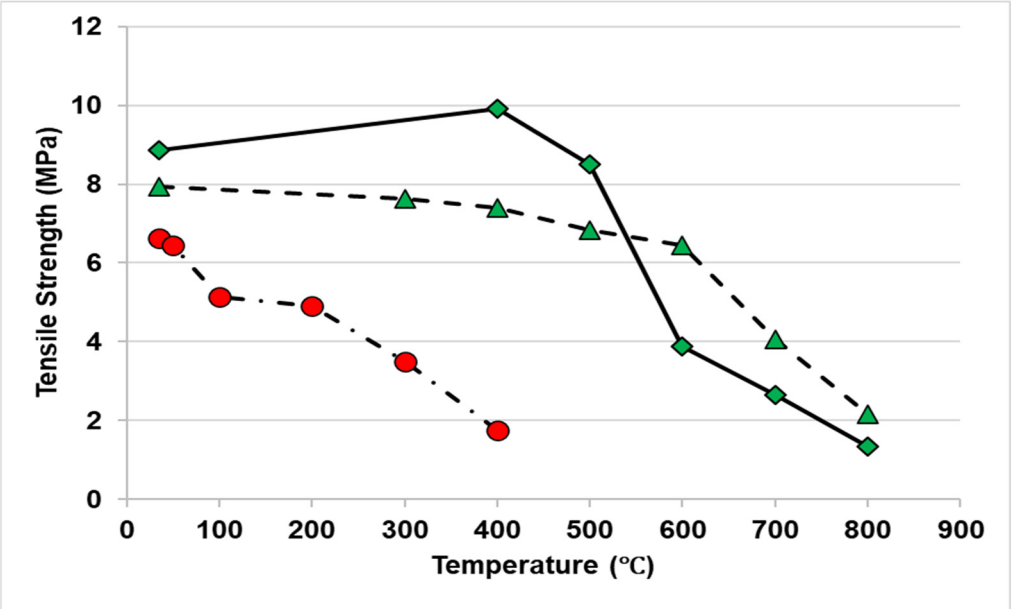

Figure 8. Tensile Strength vs. temperature. Different symbol lines represent datas from ref [1].

Table 9. Compressive Strength (MPa) of Granite.

Peak Stress															
Ref No.	Granite Type	Temperature (°C)													
		25	30	35	50	100	200	300	400	500	600	700	800	900	1000
[1]		130.11				134.1	118.26	111.85	105.54	93.11	58.21				
[5]		80.06					90.19	102.04	81.73	72.28	55.59	27.7	15.35		
[7]		215.97				190.63	234.02		203.66		119.56		96.01	38.53	37.07
[10]		120.94				135.13	133.21	121.55	95.61	74.1	50.54	22.43	15.03		

4. p-Wave Velocity–Effect of Temperature on Dynamic Properties

p-wave velocity is a dynamic property of rocks that has a relationship with density and can be determined by a non-destructive method. p-wave velocity is very useful in establishing dynamic modulus of elasticity and is widely used in rocks/structural engineering. The relationship between the p-wave velocity and other mechanical properties of rock is pre-

sented through models for rocks [38,61]. The p-wave velocity can be classified as: less than 2.5 km/s—very low, 2.5 to 3.5 km/s—low, 3.5 to 4 km/s—moderate, 4 to 5 km/s—high, and greater than 5 km/s—very high [39]. The equation for the measurement of p-wave velocity is presented as

$$v_p = \frac{L}{\Delta t} \quad (6)$$

v_p represents p-wave velocity, L is the length of the sample or core, and Δt is the travel time of the ultrasonic signal pulse between both ends of the sample [40].

The p-wave velocity generally drops due to an increase in temperature [2]. The temperature effects which change the internal structure of granite are directly dependent on the p-wave velocity of rocks.

p-wave velocity can be used as an indicator of the degree of damage of granite on heating. The standard deviation of p-wave velocity has been observed to be low in the case before the thermal treatment process [1]. The p-wave velocity decreases with an increase in temperature, and the rate of decrease is more in the case of the quenching method than in the slow-cooling method. It was observed that the rate of decreasing of p-wave velocity from 25 °C to 50 °C was around 6.8% and 14.98% in temperature from 50 °C to 100 °C. The main reason for the decrease is due to pore volume increase with rising temperature and primary crack propagation due to free water evaporation. However, due to an increase in temperature, the molecules of granite expand, and the number of cracks reduces; hence, the rate of p-wave velocity drops gradually [2]. Fan et al. [41] analyzed the geophysical properties of granite with scanning electron microscopic up to 800 °C to study the change of density and also observed the p-wave velocity and dynamic energy changes of the minerals. It was observed that with p-wave velocity, the internal structure of the rock becomes more complicated, and the rock is progressively damaged under the rising temperature [3]. Timo Saksala and Adnan Ibrahimbegovic have carried out an experiment under the dynamic loading of granite. Thermo mechanical problem is solved by analysis of 3D numerical finite element problem. The predicted and experimented thermal shock effect has good agreement with the dynamic behavior of granite. Table 10 and Figure 9 show the values and comparative analysis of primary wave velocity with an increase in temperature in the literature. It is found that the rate of primary velocity of granite decreases with increasing temperature.

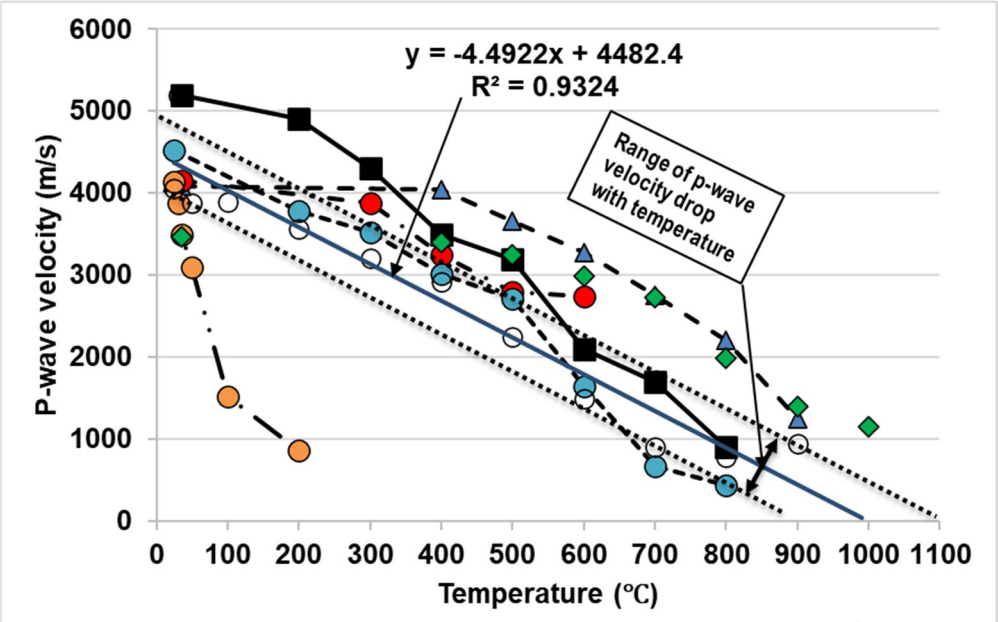

Figure 9. p-wave velocity (m/s) of Granite. Different symbol lines represent data from refs. [1–5,9].

The temperature effect on basic mechanical and physical properties was investigated by researchers in day to day. The heat treatment changes the mineral composition and pore water content in the rocks. The scanning electron microscopic test is the most important to determine the changes in crack growth [62–65].

Table 10. P-wave velocity (m/s) of Granite. The surface crack of granite material and p-wave velocity depends on the no. of cycle of temperature treatment proses [66].

P-wave															
Ref No.	Granite Type	Temperature (°C)													
		25	30	35	50	100	200	300	400	500	600	700	800	900	1000
[1]		4086.6				4036.66	3665.6	3281.66	2755.3	2205.6	1241.3				
[2]		4156.7			3873.11	3250.32	2791.81	2746.34							
[3]		3473.6				3403.1	3249.7	2983.1	2724.1	1989.6	1392.4	1155.5	1124.4	944.8	
[4]			5200			4900	4300	3500	3200	2100	1700	900			
[5]		4517					3781	3517	3020	2717	1651	670	441		
[9]						4142.32	3944.84	3883.98	3489.2	3094.41	1519.36	858.93			
[23]		3796					3849.33		3895.67		3865.00		3812.33		

Figure 9 shows that, except for reference [9], the rest of the data presented [1–5] not only behave in a logical manner but follow a close range of changes. Hence p-wave velocity measurements can be a better method to assess the impact of temperature on rock properties. Even the equation presented in Figure 9 can also be used to have a good estimate of the p-wave velocity change with temperature. The method has the advantage that it can be applied easily and in a non-destructive manner.

5. Effect of Temperature on Thermal Properties

Thermal properties are the most important parameters for design and analysis in the geothermal engineering field. The impact of temperature on such properties as in the available literature is presented below.

5.1. Thermal Damages and Thermal Cracking

Granite has a high melting point of about 2200 °C that justifies its use in multiple purposes applications. Although it has a huge heat resistance capability even in the range of 250 °C to 650 °C, the temperature still affects the physical and mechanical properties of granite.

The mass loss takes place due to the evaporation of water particles from the crystal lattice when granite is heated up to 600 °C [31]. The basic structural changes would occur between 300 °C to 600 °C, which represents the brittle to ductile state [42] of the rock. Temperature induces micro-cracks that are broadly observed at a temperature of 800 °C. The micro-cracks thus generated an effect on the shear fracture properties and reduced the fracture toughness of the rock [30]. The thermal damages basically occur due to heat expansion of mineral and thermo-elastic moduli of rocks [43]. The thermal damages occur from a certain thermal shock on granite. This shock damages and fractures the material permanently.

The enlargement and transfixion effects on the internal structure of granite due to temperature changes and evaporation of free water result in damage to the surface of granite [2]. The surface color of granite changes due to changes in temperature, oxidation, phase changes, and mineral structure. Due to temperature changes, cracks develop rapidly in the rock sample, which leads to a change in mechanical and physical properties [3]. The cleavage fracture changes due to an increase in temperature. The thermo-mechanical stress factor also depends on the thermal damages due to mechanical force and temperature changes. The thermal damage of rocks is represented as a law of the thermal plastic behavior of rocks.

$$D(T) = 1 - \frac{E_T}{E_0} \quad (7)$$

where $D(T)$ is the thermal damage, E_T is elastic modulus at high temperatures, and E_0 is the elastic modulus at room temperature.

Between 400 °C to 1000 °C, the thermal damage of granite increases, mostly [12]. The value of thermal damage varies slightly, but the change is remarkable between 100 °C to 200 °C. Due to the heating of rock, the strength is reduced, and cracks proliferate and damage the rock. The propagation of new cracks is the main reason for thermal damage. With an increase in temperature from 400 °C to 1000 °C, the thermal damages are induced sharply due to a reduction in cohesive force and movement of the particles. Hence, damage due to thermal stress becomes prominent [25,44,45]. The heterogeneity of rock surfaces is a primary reason for damage to rocks. Thermal damages basically took place on the drilling tool material while drilling at elevated temperatures. The mechanical properties of the tool's material also deteriorated at elevated temperatures. Gan Feng et al. have discussed carried out extensive experimentation on the fracture toughness behavior of granite materials. The result of the experimental study is conducive to attaining an in-depth understanding of the deep rock mechanical properties along with the exploration possibilities of hot clay rock related to reservoir construction. They have discussed that external load and thermal stresses cause damage to the rocks along the line of compaction of ore cracks. They have carried out extensive seaming electron microscope attachment and the measurement of acquisitive wave velocities to substantiate their recommendation [67]. Chun Wang et al. have discussed the static and dynamic failure behavior of the granite material subjected to the water heat cycle. The researchers have proposed that the variation of low dynamic deformation, which appeared extensively, disappears in comparison to the changes in static appears deformation. Based on those dynamic failure criteria with the consideration of the crack along the loading direction were generated. They have verified the result with the relevant standard testing procedure [68]. Liyuan et al. have discussed the dual damage constitutive model to elaborately explain thermal damage in rock materials. They are studied in relation to the development of the dual damage's activities model to critically varying thermomechanical damage processes related to thermal treatment. This methodology considered damage variables to separately alter the elastic modulus and strength of the rock materials. They have concluded that, with an increase in temperature, the elastic modulus and strength decrease. If the deep is higher than the elastic modulus and strength of the rock will be lower [69]. Chengkang Mo et al. have described the real-time measurement of the mechanical characteristic of granite material at the time of experiencing the heating and cooling cycle [70]. Li Yu et al. have discussed the thermal shock generation during water cooling of heated granite under thermal treatment at a temperature of 300 °C. They studied the pores and crack generation of granite [71]. Qiang Li et al. [72] have conducted an experiment to investigate thermal damage with the help of a magnetic resonance imaging test and heat conduction test. Jonas Enzell and Markus Tollisten [73] investigated the cracking phenomenon in a concrete dam with seasonal temperature variation. The reduction of oxidation is one of the key factors of convectional concrete materials. The analysis of chemical bonding and physical and mechanical characteristics are most important to evaluate the physical phenomenon of the materials [74]. Table 11 shows the values of thermal damages with temperature by different authors.

Table 11. Thermal damages.

Porosity															
Ref No.	**Granite Type**	**Temperature (°C)**													
		25	**30**	**35**	**50**	**100**	**200**	**300**	**400**	**500**	**600**	**700**	**800**	**900**	**1000**
[2]		0			0.07	0.25	0.34								
[3]		0.07				0.11	0.19	0.31	0.43						
[15]	Jalore	0					0.0817	0.454	0.605	0.739	0.86				

Figure 10 shows the analysis of thermal damages for different research papers with respect to temperature changes. It is observed that due to the change in temperature, different studies' thermal damages increased in a linear fashion, as shown in Table 11 and Figure 10.

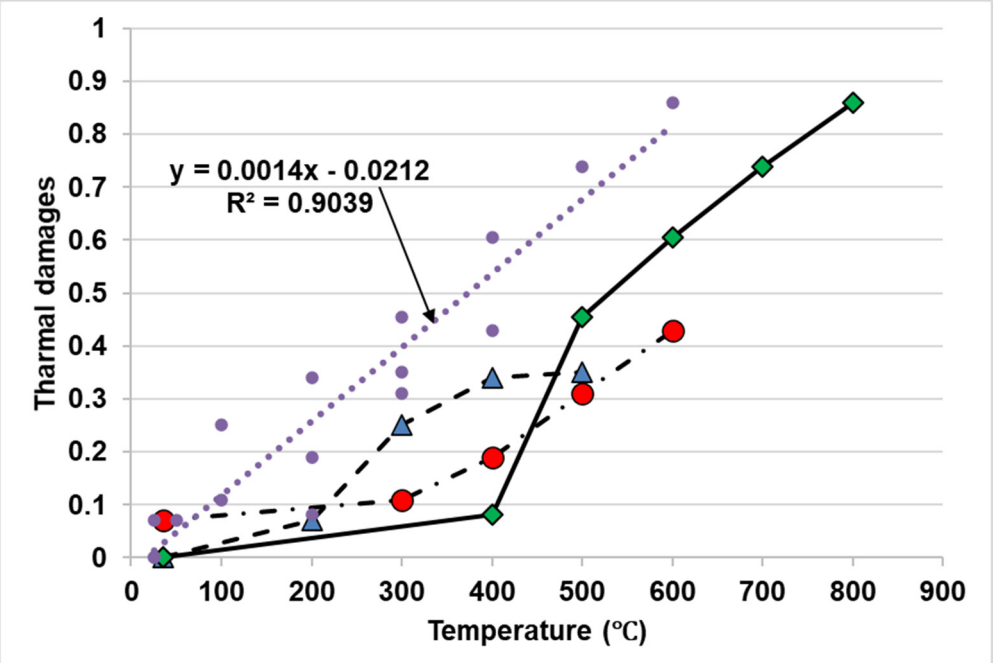

Figure 10. Thermal damages vs. temperature. Different symbol lines represent data from refs. [2,3,15].

The thermal damages correlate well with the temperature and can also be used as a method for determining the effect of temperature on a rock. The equation presented in Figure 10 can also be used to estimate such damages as R^2 of the equation is quite high.

5.2. Thermal Conductivity and Diffusivity

Thermal conductivity is a material property that involves the transport and exchange of thermal energy. It is a measure of the rate of heat loss and temperature distribution for the formation of rocks [46]. Kent et al. [47] observed that the thermal conductivity and diffusivity of granite decrease about 75% of the initial value when heated from 25 °C to 500 °C and is mainly due to the reduction of water molecules present in the material [48]. Durham et al. [49] compared the thermal diffusivity of different granite samples from 30 °C to 400 °C. It was observed that the Stripa Granite has the highest thermal diffusivity than the Beishan granites. The thermal diffusivity varies inversely with temperature. The thermal conductivity decreases from about 40% to 60% with an increase in temperature up to 900 °C [50]. The main reason of decrease of thermal conductivity and diffusivity due to the development of crack generation between 200 °C to 300 °C and due to phase transformation in quartz at 500 °C to 600 °C [51]. Thermal conductivity inherently depends on temperature treatment and the quenching cycle. The thermal conductivity generally decreases as the temperature rises [66]. Zheng-Wei-Li et al. [75] conducted heat treatment on granite up to 1000 °C temperature and cooled the sample with air and water, respectively. They measured the thermal conductivity distribution with the help of the optical scanning method. They have observed that thermal conductivity decreases by about 54% after heating at 1000 °C. The thermal conductivity decrease rate is higher in the water-cooled sample than in the air-cooled sample.

5.3. Specific Heat

The specific heat of granite increases with temperature from 25 °C to 80 °C, about 15% of the initial value [48]. Miao et al. [50] observed that specific heat increases with temperature up to 900 °C, and specific heat has a reverse effect on the decrease of thermal conductivity. Sun et al. [51] examined the effect of specific heat up to 900 °C. The temperature was divided into three stages, i.e., stage I (25 °C to 300 °C), stage II (400 °C to 600 °C), and stage III (700 °C to 900 °C). It was observed that up to 300 °C the specific heat is very low, and after that, it increased to about 0.6 J/(kg × k), and after 700 °C it increased more than the lower temperature, and at 900 °C the value was 0.68 J/(kg × k). Xiaoqi Wang et al. [76] describe the storage of energy and oxidation of broken coal during gas removal. The correlation between temperature and mechanical characteristics was analyzed. Yu-Fu et al. [77] presented a numerical model to analyze the thermomechanical behavior of brittle materials and the relationship between temperature and mechanical properties of materials. Mohammod-Taghi et al. [78] conducted research on seven different natural building rocks to analyze the mechanical and physical performance of materials.

6. Analysis of the Work

6.1. Significance of the Work

Actual work is very much crucial and significant for granite drilling activity. The drilling of granite is always encountering the problem of profuse heat generation. This exorbitant heat will deform the outer surface of the drilling tool and make it soft due to this effect. The soft tool cannot drill further and becomes further deformed by the surrounding granite material. A lubricant or cooling agent, such as water, cannot take away the generated heat easily from the surface of the drilling tool, i.e., the affectivity of the drilling process is compromised to a great extent, and the progress of drilling substantially reduced. Some hot resistance material like tungsten carbide is used in the peripheral position of the drilling tool, but those materials also have limited hot hardness after reaching temperatures from 600 °C to 700 °C. Because of this inherent limitation, the drilling of rock mass is always a challenging option for the user to attend a good level of productivity in a rock drilling operation. The present review article emphasizes the critical understanding of the thermal profile in the neighborhood of drilling tools to effectively implement and monitor drilling operations. If the appropriate comprehension of the analysis of the thermal environment is created during drilling, efficient and productive drilling cannot be achieved. Very few articles are presently available to describe the challenges of negotiating the profuse heat generation in specific drilling operations of granite material. As this granite rock mass is an extensive industrial application, the systematic in-depth understanding of the entire heat generation phenomena of granite drilling is of extreme importance. In many cases, due to the lack of knowledge of the thermal behavior, the speed of drilling is implemented to obtain higher productivity. However, in the end, the progress rate of the drilling is greatly reduced because of the profuse heat generation and subsequent deformation of the drilling tool at the edges responsible for the drilling activity. Therefore, a well-structured, well-documented review article is very much necessary for the practicing engineers to carry out efficient, effective, time bound, goal oriented drilling of granite materials.

6.2. Standardization of the Work

In order to standardize the different values of different levels of drilling for various heat generations, a detailed table has been incorporated in the manuscript. The tangible values of the different levels of temperature generated at the time of drilling granite materials have been meticulously represented so that it is comprehensive even for a layman to operate drilling activities confidently for a special case of granite materials. The graphs related to the generation of temperature will manifest the thermal behavior pictorial to the reader of the article. The graphical representation of the thermal profile is a cognate approach to make the user aware of the various level of temperatures generated at the peripheral surface of the drilling tool. The reader will also appropriate the incapability of a cooling agent,

like water, to take away the unwanted heat from the drilling tool for efficient progress in operation. The tabular and graphical representations are documentary evidence of the standardized assessment of the thermal characteristic in the relevant domain knowledge.

6.3. Heat Treatment on Cutting Tool Related to Rock Mass

Usually, the tungsten carbide is used for the drilling activity of abrasive and hard rock mass. Tungsten carbide has an appreciably high value of hot hardness and hot strength. Because of this characteristic, the use of tungsten carbide in rock drilling is a gain changer. For this reason, the drilling tool consisting of tungsten carbide has much better performance in comparison to the traditional steel tool for rock drilling activities. The tungsten particle needs appropriate heat treatment to the weighted heat carbon particle in the special heat treatment process. The efficiency of this heat treatment process performed on the drilling tool will ensure the efficiency of rock drilling activity. Tungsten carbide material also has high hot strength, i.e., it will also retain its strength at elevated temperatures. However, the hot hardness and hot strength as also limited values, and that cannot be effective in a temperature beyond 1000 °C. For this reason, the practicing engineer has to understand the critical thermal behavior and thermal damage caused to the drill bit while drilling at an elevated temperature.

6.4. Some Prospective Non-Traditional Drilling Techniques for Granite Materials

There is a lot of development in terms of enhancing the drillability of granite and other rock material through non-traditional processes. One of the most popular non-conventional processes of rock cutting is the use of a high-pressure water jet. The pressure, from 200 MPa to 300 Mpa, is used to make drill holes in rock materials. The beauty of the process is that there is no possibility of the generation of heat as the water is used both as the tool of drilling as well as the coolant. Some of the researchers used pulsating water jets for rock mass disintegration with a lower value of water pressure in comparison with the continuous water jet. A pulsating water jet uses a self-seasonality nozzle in order to create pulsation. The water jet drilling of rock mass is a game-changing technology. The water of the high-pressure water jet suppresses the suspended particle generated out of the rock drilling activity. This is a very user-friendly process as there are minimum health hazards because of the auto deist suppressing character of the process. Yang Zengqiang et al. [79] described a water jet process in a weak structure zone of rocks. The continuous stress of superposition forms when drilling with a water jet, and the load is distributed to surrounding rocks.

An abrasive water jet is also used for the drilling of granite materials. The suspended abrasive acts as a numerous machine tool and ensures stress-free removal of materials from the workpiece. Yiyu Lu et al. [80] developed an abrasive water jet machine for drilling hard rock by introducing the 'boss' to generate a 'pilot hole' for resistance of shear, tensile strength, as well as compressive strength.

Ultrasonic drilling is also a good option for drilling activities in granite materials. Granite, as well as other rock materials, have very low shock-absorbing capacity. Therefore, when ultrasonic excitation with a probe is provided very fast, efficient material removal is achieved. Rupam Tripathi et al. [81] presented an acoustic emission technique to drill out the rock with a non-conventional process to prevent rock deterioration. This phenomenon is extensively applied to the drilling activities of ceramic materials.

7. Conclusions

This paper presents a review of the effect of the thermal treatment of granite. The impact of temperature and cooling conditions on various physical, mechanical, and thermal properties used by various authors have been summarized and analyzed critically to evaluate a holistic view of the impact of temperature treatment on granite. The following conclusion can be drawn based on the work:

1. The stress of granite decreases mildly with an increase of temperature up to 400 °C, beyond which the stress decreases rapidly. The strain increases about three times when heated from room temperature to 1000 °C.
2. The density of granite after heat treatment decreases. The density decrease rate in the rapid-quenching process is lower than in the slow cooling process due to the absorption of some moisture content. Despite of initial average density of 2628 kg/m^3 and a standard deviation of a mere 13 kg/m^3 observed in the literature cited, there is increasing variation ranging from 33 to 242 kg/m^3 in density after heat treatment up to 600 °C. This has a significant connotation in terms of methods deployed for such tests and calls for more controlled testing or better test methods. The reports of such density variations should invariably provide comprehensive detail of the rock properties in terms of mineralogy and petrology.
3. The porosity increases with an increase in temperature. The permeability decreases with an increase in temperature due to the reactivity of material at high temperatures. However, the data on this property is limited.
4. The compressive strength shows little change up to 400 °C, beyond which, in most cases, shows a steep drop. The tensile strength behaves in a different manner in the cases examined but shows a significant drop in its values up to 800 °C. Young's Modulus decreases with temperature and has a huge variability which needs to be ascertained through exhaustive information on the granites analyzed. Poisson's ratio initially decreases up to 600 °C then increase rapidly up to 800 °C. Compressive strength and Tensile strength both decrease with an increase in temperature.
5. The p-wave velocity decreases due to the pore volume of material increasing with rising temperature. The p-wave not only behaves in a logical manner but follows a close range in changes over temperature. Hence p-wave velocity can be a better descriptor to assess the impact of temperature on rock properties. Even the equation presented in Figure 9 can be used to estimate the p-wave velocity change with temperature. The method has the advantage that it can be applied easily and in a non-destructive manner.
6. Thermal damages also show a steep increase with an increase in temperature. This method is difficult to adopt but shows a very good trend with increasing temperature, as shown in Figure 10; the relation given therein can be used to estimate thermal damages due to an increase in temperature.
7. Thermal conductivity and thermal diffusivity decrease by 60% to 75% up to 900 °C due to crack development and phase transformation of quartz. The specific heat of granite increases with an increase in temperature.
8. There is a strong need to standardize the test methods. P-wave velocity and thermal damages are good candidates for this purpose and need to be further evaluated to check their veracity for such purposes.
9. Hence, this review paper will be greatly beneficial to the future researcher to find out the relevant research gap and carry out related research for useful implementation.

Author Contributions: Conceptualization, S.P., S.C., A.K.R., S.S., C.L. and Y.Z.; formal analysis, S.P., S.C., A.K.R., S.S., C.L., Y.Z. and A.K.; investigation, S.P., S.C., A.K.R., S.S., C.L. and Y.Z.; writing—original draft preparation, S.P., S.C., A.K.R., S.S., C.L. and Y.Z.; writing—review and editing, S.S., A.K. and E.T.-E.; supervision, S.S. and E.T.-E.; project administration, S.S. and E.T.-E.; funding acquisition, S.S. and E.T.-E. All authors have read and agreed to the published version of the manuscript.

Funding: This research received no external funding.

Institutional Review Board Statement: Not applicable.

Informed Consent Statement: Not applicable.

Data Availability Statement: Not applicable.

Acknowledgments: This paper is a part of the Ph.D. work of the first author. Thanks are due to heads of various organizations to which the authors belong for their permission to publish the paper.

Conflicts of Interest: The authors declare no conflict of interest.

Abbreviations

σ	Peak stress
σ_1	Initial stress of material
σ_2	Terminated stress of material
T	Temperature.
ϵ	Strain.
ε_1	Initial strain of material.
ε_2	Terminated strain of material.
∅	Porosity of rocks.
V_{pores}	Volume of void space
V_{rock}	Total bulk volume of rock.
E	Elastic modulus
E_T	Elastic modulus at high temperature.
E_o	Elastic modulus at room temperature
μ	Poisson's ratio.
P	Density of the material.
ν	Longitudinal wave velocity of the material.
v_p	p-wave velocity.
L	Length of cylindrical rods.
Δt	Travel time of signal pulse between both ends.
$D(T)$	Thermal damages.

References

1. Jina, P.; Hua, Y.; Shaoa, J.; Zhaoa, G.; Zhua, X.; Lia, C. Influence of different thermal cycling treatments on the physical, mechanical and transport properties of granite. *Geothermics* **2019**, *78*, 118–128. [CrossRef]
2. Yin, T.-B.; Shu, R.-H.; Li, X.-B.; Wang, P.; Dong, L.-J. Combined effects of temperature and axial pressure on dynamic mechanical properties of granite. *Trans. Nonferrous Met. Soc. China* **2016**, *26*, 2209–2219. [CrossRef]
3. Zhu, S.; Zhang, W.; Sun, Q.; Deng, S.; Geng, J.; Li, C. Thermally induced variation of primary wave velocity in granite from Yantai: Experimental and modeling results. *Int. J. Therm. Sci.* **2017**, *114*, 320–326. [CrossRef]
4. Su, G.; Chen, Z.; Ju, J.W.; Jian, J. Influence of temperature on the strainburst characteristics of granite under true triaxial loading conditions. *Eng. Geol.* **2016**, *222*, 38–52. [CrossRef]
5. Yang, S.-Q.; Ranjith, P.G.; Jing, H.-W.; Tian, W.-L.; Ju, Y. An experimental investigation on thermal damage and failure mechanical behavior of granite after exposure to different high temperature treatments. *Geothermics* **2017**, *65*, 180–197. [CrossRef]
6. Shao, S.; Ranjith, P.G.; Wasanth, P.L.P.; Chen, B.K. Experimental and numerical studies on the mechanical behaviour of Australian Strathbogie granite at high temperatures: An application to geothermal energy. *Geothermics* **2015**, *54*, 96–108. [CrossRef]
7. Kumari, W.G.P.; Ranjith, P.G.; Perera, M.S.A.; Chen, B.K.; Abdulagatov, I.M. Temperature-dependent mechanical behaviour of Australian Strathbogie granite with different cooling treatments. *Eng. Geol.* **2017**, *229*, 31–44. [CrossRef]
8. Nasseri, M.H.B.; Schubnel, A.; Young, R.P. Coupled evolutions of fracture toughness and elastic wave velocities at high crack density in thermally treated Westerly granite. *Int. J. Rock Mech. Min. Sci.* **2007**, *44*, 601–616. [CrossRef]
9. Chaki, S.; Takarli, M.; Agbodjan, W.P. Influence of thermal damage on physical properties of a granite rock: Porosity, permeability and ultrasonic wave evolutions. *Constr. Build. Mater.* **2008**, *22*, 1456–1461. [CrossRef]
10. Du, S.J.; Liu, H.; Zhi, H.T. Testing study on mechanical properties of post -high-temperature granite. *Chin. J. Rock Mech. Eng.* **2004**, *14*, 2359–2364. (In Chinese)
11. Jianxin, H.A.N.; Shucai, L.I.; Shuchen, L.I.; Lei, W. Post-peak Stress-strain Relationship of Rock Mass Based on Hoek-Brown Strength Criterion. *Procedia Earth Planet. Sci.* **2012**, *5*, 289–293. [CrossRef]
12. Gautam, P.K.; Verma, A.K.; Jha, M.K.; Maheshwar, S.; Singh, T.N. Effect of high temperature on physical and mechanical properties of granite. *J. Appl. Geophys.* **2017**, *159*, 30140–30144. [CrossRef]
13. Isaka, B.A.; Ranjith, P.; Rathnaweera, T.; Perera, M.; De Silva, V. Quantification of thermally-induced microcracks in granite using X-ray CT imaging and analysis. *Geothermics* **2019**, *81*, 152–167. [CrossRef]
14. Vagnona, F.; Colombero, C.; Colombo, F.; Comina, C.; Ferrero, A.M.; Mandrone, G.; Vinciguerra, S.C. Effects of thermal treatment on physical and mechanical properties of Valdieri Marble—NW Italy. *Int. J. Rock Mech. Min. Sci.* **2019**, *116*, 75–86. [CrossRef]
15. Homand-Etienne, F.; Houpert, R. Thermally Induced Microcracking in Granites: Characterization and Analysis. *Int. J. Rock Mech. Win. Sci. Geomech. Abstr.* **1989**, *26*, 125–134. [CrossRef]
16. Shan, Y.; Zhao, J.; Tong, H.; Yuan, J.; Lei, D.; Li, Y. Effects of activated carbon on liquefaction resistance of calcareous sand treated with microbially induced calcium carbonate precipitation. *Soil Dyn. Earthq. Eng.* **2022**, *161*, 107419. [CrossRef]

17. Xu, X.L.; Feng, G.A.; Shen, X.M.; Xie, H.P. Mechanical characteristics and microcosmic mechanisms of granite under temperature loads. *J. China Univ. Min. Technol.* **2008**, *18*, 0413–0417. [CrossRef]
18. Chen, Y.; Hu, S.; Wei, K.; Hu, R.; Zhou, C.; Jing, L. Experimental characterization and micro mechanical modeling of damage-induced permeability variation in Beishan granite. *Int. J. Rock Mech. Min. Sci.* **2014**, *71*, 64–76. [CrossRef]
19. Chen, S.; Yang, C.; Wang, G. Evolution of thermal damage and permeability of Beishan granite. *Appl. Therm. Eng.* **2017**, *110*, 1533–1542. [CrossRef]
20. Moore, D.E.; Lockner, D.A.; Byerlee, J.D. Reduction of Permeability in Granite at Elevated temperatures. *Science* **1994**, *265*, 1558–1561. [CrossRef]
21. Siratovich, P.A.; Villeneuve, M.C.; Cole, J.W.; Kennedy, B.M.; Bégué, F. Saturated heating and quenching of three crustal rocks and implications for thermal stimulation of permeability in geothermal reservoirs. *Int. J. Rock Mech. Min. Sci.* **2015**, *80*, 265–280. [CrossRef]
22. Aim, O.; Jaktlund, L.; Shaoquan, K. The influence of microcrack density on the elastic and fracture mechanical properties of Stripa granite. *Phys. Earth Planet. Inter.* **1985**, *40*, 161–179.
23. Kang, F.; Jia, T.; Li, Y.; Deng, J.; Tang, C.; Huang, X. Experimental study on the physical and mechanical variations of hot granite under different cooling treatments. *Renew. Energy* **2021**, *179*, 1316–1328. [CrossRef]
24. Heuze, F.E. High-temperature Mechanical, Physical and Thermal Properties of Granitic Rocks. A Review. *Int. J. Rock Mech. Min. Sci. Geomech. Abstr.* **1983**, *20*, 3–10. [CrossRef]
25. Liu, S.; Xu, J. Mechanical properties of Qinling biotite granite after high temperature treatment. *Int. J. Rock Mech. Min. Sci.* **2014**, *71*, 188–193. [CrossRef]
26. Yin, T.-B.; Shu, R.-H.; Li, X.-B.; Wang, P.; Liu, X.-L. Comparison of mechanical properties in high temperature and thermal treatment granite. *Trans. Nonferrous Met. Soc. China* **2016**, *26*, 1926–1937. [CrossRef]
27. Chen, Y.-L.; Wang, S.-R.; Jing, N.; Azzam, R.; Tomás, M.; Fernández, S. An experimental study of the mechanical properties of granite after high temperature exposure based on mineral characteristics. *Eng. Geol.* **2016**, *220*, 234–242. [CrossRef]
28. Wu, X.; Huang, Z.; Cheng, Z.; Zhang, S.; Song, H.; Zhao, X. Effects of cyclic heating and LN2-cooling on the physical and mechanical properties of granite. *Appl. Therm. Eng.* **2019**, *156*, 99–110. [CrossRef]
29. Yang, S.; Tian, W.; Huang, Y. Failure mechanical behavior of pre-holed granite specimens after elevated temperature treatment by particle flow code. *Geothermics* **2018**, *72*, 124–137. [CrossRef]
30. Zhao, Z.; Dou, Z.; Xu, H.; Liu, Z. Shear behavior of Beishan granite fractures after thermal treatment. *Eng. Fract. Mech.* **2019**, *213*, 223–240. [CrossRef]
31. Zuo, J.; Wang, J.; Sun, Y.; Chen, Y.; Jiang, G.; Li, Y. Effects of thermal treatment on fracture characteristics of granite from Beishan, a possible high-level radioactive waste disposal site in China. *Eng. Fract. Mech.* **2017**, *182*, 425–437. [CrossRef]
32. Chang, C.; Zoback, M.D.; Khaksar, A. Empirical relations between rock strength and physical properties in sedimentary rocks. *J. Pet. Sci. Eng.* **2006**, *51*, 223–237. [CrossRef]
33. Walsh, J.B. The effect of cracks on the compressibility of rock. *J. Geophys. Res.* **1965**, *70*, 381–389. [CrossRef]
34. David, E.C.; Brantut, N.; Schubnel, A.; Zimmerman, R.W. Sliding crack model for nonlinearity and hysteresis in the uniaxial stress–strain curve of rock. *Int. J. Rock Mech. Min. Sci.* **2012**, *52*, 9–17. [CrossRef]
35. ISRM. *The Complete ISRM Suggested Methods for Rock Characterisation, Testing and Monitoring: 1974–2006*; ISRM Commission on Testing Methods: Ankara, Turkey, 2007.
36. Yang, S.Q.; Jing, H.W.; Huang, Y.H.; Ranjith, P.G.; Jiao, Y.Y. Fracture mechanical behavior of red sandstone containing a single fissure and two parallel fissures after exposure to different high temperature treatments. *J. Struct. Geol.* **2014**, *69*, 245–264. [CrossRef]
37. Yang, S.Q.; Ranjith, P.G.; Huang, Y.H.; Yin, P.F.; Jing HWGui, Y.L.; Yu, Q.L. Experimental investigation on mechanical damage characteristics of sandstone under tri axial cyclic loading. *Geophys. J. Int.* **2015**, *201*, 662–682. [CrossRef]
38. Saffet, Y. P-wave velocity test for assessment of geotechnical properties of some rock materials. *Bull. Mater. Sci.* **2011**, *34*, 947–953.
39. Anon, O.H. Classification of rocks and soils for engineering geological mapping. Part 1: Rock and soil materials. *Int. Ass. Eng. Geol. Bull.* **1979**, *19*, 364–437.
40. Mustaqim, M.M.; Zainab, M. Empirical Correlation of P-wave Velocity to the Density of Weathered Granite. In Proceedings of the International Civil and Infrastructure Engineering Conference, Kuching, Malaysia, 22–25 September 2013; pp. 22–24.
41. Fan, L.F.; Wu, Z.J.; Wan, Z.; Gao, J.W. Experimental investigation of thermal effects on dynamic behavior of granite. *Appl. Therm. Eng.* **2017**, *125*, 94–103. [CrossRef]
42. Sun, Q.; Zhang, W.; Xue, L.; Zhang, Z.; Su, T. Thermal damage pattern and thresholds of granite. *Environ Earth Sci.* **2015**, *74*, 2341–2349. [CrossRef]
43. Kranz, R.L. Microcracks in rocks: A review. *Tectonophysics* **1983**, *100*, 449–480. [CrossRef]
44. Liu, S.; Xu, J.Y. Study on dynamic characteristics of marble under impact loading and high temperature. *Int. J. Rock Mech. Min. Sci.* **2013**, *62*, 51–58. [CrossRef]
45. Liu, S.; Xu, J. An experimental study on the physico-mechanical properties of two post-high temperature rocks. *Eng. Geol.* **2014**, *185*, 63–70. [CrossRef]
46. Cho, W.J.; Kwon, S.; Choi, J.W. The thermal conductivity for granite with various water contents. *Eng. Geol.* **2009**, *107*, 167–171. [CrossRef]

47. Kant, M.A.; Ammann, J.; Rossi, E.; Madonna, C.; Höser, D.; von Rohr, P.R. Thermal properties of Central Aare granite for temperatures up to 500°C: Irreversible changes due to thermal crack formation. *Geophys. Res. Lett.* **2016**, *44*, 771–776. [CrossRef]
48. Cho, W.; Kwon, S. Estimation of the thermal properties for partially saturated granite. *Eng. Geol.* **2010**, *115*, 132–138. [CrossRef]
49. Durham, W.B.; Mirkovich, V.V.; Heard, H.C. Thermal Diffusivity of Igneous Rocks at Elevated Pressure and Temperature. *J. Geophys. Res.* **1987**, *92*, 11615–11634. [CrossRef]
50. Miao, S.; Li, H.P. Temperature dependence of thermal diffusivity, specific heat capacity, and thermal conductivity for several types of rocks. *J. Therm. Anal. Calorim.* **2013**, *115*, 1057–1063. [CrossRef]
51. Sun, Q.; Zhang, W.; Zhu, Y.; Huang, Z. Effect of High Temperatures on the Thermal Properties of Granite. *Rock Mech. Rock Eng.* **2019**, *52*, 2691–2699. [CrossRef]
52. Zhu, Z.; Tian, H.; Mei, G.; Jiang, G.; Dou, B.; Xiao, P. Experimental investigation on mechanical behaviors of Nanan granite after thermal treatment under conventional triaxial compression. *Environ. Earth Sci.* **2021**, *80*, 46. [CrossRef]
53. Du, G.; Chen, S.; Chen, X.; Jiang, Z. Temperature damage regularity of granite based on micro-inhomogeneity. 2022. Available online: https://www.frontiersin.org/journals/earth-science (accessed on 10 August 2021).
54. Zhu, D.; Fan, Y.; Miao, L.; Jin, H.; Jing, H.; Liu, X. Study of tensile mechanical properties of granite after repeated action of high temperature-water cooling. 2022; *preprint*. [CrossRef]
55. Meng, X.; Liu, W.; Meng, T. Experimental Investigation of Thermal Cracking and Permeability Evolution of Granite with Varying Initial Damage under High Temperature and Triaxial Compression. *Adv. Mater. Sci. Eng.* **2018**, *2018*, 8759740. [CrossRef]
56. Xu, J.; Kang, Y.; Wang, Z.; Wang, X.; Zeng, D.; Su, D. Dynamic Mechanical Behavior of Granite under the Effects of Strain Rate and Temperature. *ASCE Int. J. Géoméch.* **2020**, *20*, 1–12. [CrossRef]
57. Wu, Z.; Xu, J.; Li, Y.; Wang, S. Disturbed State Concept–Based Model for the Uniaxial Strain-Softening Behavior of Fiber-Reinforced Soil. *Int. J. Geomech.* **2022**, *22*, 4022092. [CrossRef]
58. Chen, K.; Guo, Z.; Zhu, C. Study on Mechanical Properties and Damage Evolution Law of Granite after High Temperature Cooling. In *IOP Conference Series: Earth and Environmental Science*; IOP Publishing: Bristol, UK, 2020; Volume 455. [CrossRef]
59. Tomas, R.; Cano, M.; Pulgarín, L.F.; Brotons, V.; Benavente, D.; Miranda, T.; Vasconcelos, G. Thermal effect of high temperatures on the physical and mechanical properties of a granite used in UNESCO World Heritage sites in north Portugal. *J. Build. Eng.* **2021**, *43*, 102823. [CrossRef]
60. Saksala, T. 3D Numerical Prediction of Thermal Weakening of Granite under Tension. *Geosciences* **2021**, *12*, 10. [CrossRef]
61. Saksala, T.; Ibrahimbegovic, A. Thermal shock weakening of granite rock under dynamic loading: 3D numerical modeling based on embedded discontinuity finite elements. *Int. J. Numer. Anal. Methods Géoméch.* **2020**, *44*, 1788–1811. [CrossRef]
62. Yang, J.; Fu, L.; Fu, B.; Deng, W.; Han, T. Third-Order Padé Thermoelastic Constants of Solid Rocks. *J. Geophys. Res. Solid Earth* **2022**, *127*, e2022J–e24517J. [CrossRef]
63. Fang, X.; Xu, J.; Liu, S.; Wang, H. Influence of Heating on Tensile Physical-Mechanical Properties of Granite. *High Temp. Mater. Proc.* **2019**, *38*, 505–515. [CrossRef]
64. Xiao, Y.; Zhao, R.; Huang, Q.; Deng, J.; Lu, J. Numerical tests on thermal cracking characteristics of rocks with different scales. *Adv. Mech. Eng.* **2018**, *10*, 1–11. [CrossRef]
65. Isaka, B.L.A.; Gamage, R.P.; Rathnaweera, T.D.; Perera, M.S.A.; Chandrasekharam, D.; Kumari, W.G.P. An Influence of Thermally-Induced Micro-Cracking under Cooling Treatments: Mechanical Characteristics of Australian Granite. *Energies* **2018**, *11*, 1338. [CrossRef]
66. Hu, J.; Xie, H.; Sun, Q.; Li, C.; Liu, G. Changes in the thermodynamic properties of alkaline granite after cyclic quenching following high temperature action. *Int. J. Min. Sci. Technol.* **2021**, *31*, 843–852. [CrossRef]
67. Feng, G.; Liu, C.-B.; Wang, J.-L.; Tao, Y.; Duan, Z.-P.; Xiang, W.-N. Experimental Study on the Fracture Toughness of Granite Affected by Coupled Mechanical-Thermo. *Geo Sci. World Lithosphere* **2021**, *2022*, 5715093. [CrossRef]
68. Wang, C.; Li, X.-R.; Xie, M.-Z.; Xiong, Z.-Q.; Wang, C.; Wang, H.-B.; Zhan, S.-F.; Hu, Y.-C. Static and dynamic failure mechanisms of circular granite under the condition of water-heat cycles. *Sci. Rep.* **2021**, *11*, 5927. [CrossRef]
69. Liu, L.; Ji, H.; Elsworth, D.; Zhi, S.; Lv, X.; Wang, T. Dual-damage constitutive model to define thermal damage in rock. *Int. J. Rock Mech. Min. Sci.* **2020**, *126*, 104185. [CrossRef]
70. Mo, C.; Zhao, J.; Zhang, D. Real-Time Measurement of Mechanical Behavior of Granite During Heating–Cooling Cycle: A Mineralogical Perspective. *Rock Mech. Rock Eng.* **2022**, *55*, 4403–4422. [CrossRef]
71. Yu, L.; Peng, H.; Zhang, Y.; Li, G. Mechanical test of granite with multiple water–thermal cycles. *Geotherm Energy* **2021**, *9*, 1–20. [CrossRef]
72. Li, Q.; Yin, T.; Li, X.; Shu, R. Experimental and Numerical Investigation on Thermal Damage of Granite Subjected to Heating and Cooling. *Mathematics* **2021**, *9*, 3027. [CrossRef]
73. Enzell, J.; Tollsten, M. *Thermal Cracking of a Concrete Arch Dam Due to Seasonal Temperature Variations*; KTH School of ABE: Stockholm, Sweden, 2017; ISSN 1103-4297.
74. Amran, M.; Fediuk, R.; Murali, G.; Avudaiappan, S.; Ozbakkaloglu, T.; Vatin, N.; Karelina, M.; Klyuev, S.; Gholampour, A. Fly Ash-Based Eco-Efficient Concretes: A Comprehensive Review of the Short-Term Properties. *Materials* **2021**, *14*, 4264. [CrossRef]
75. Li, Z.; Long, M.; Feng, X.; Zhang, Y. Thermal damage effect on the thermal conductivity inhomogeneity of granite. *Int. J. Rock Mech. Min. Sci.* **2021**, *138*, 104583. [CrossRef]

76. Wang, X.; Ma, H.; Qi, X.; Gao, K.; Li, S.; Yang, X. Experimental study on the effect of hightemperature oxidation coal mechanical characteristics. *PLoS ONE* **2022**, *17*, e0264039. [CrossRef]
77. Fu, Y.; Wang, Z.; Ren, F.; Wang, D. Numerical model of thermo-mechanical coupling for the tensile failure process of brittle materials. *AIP Adv.* **2017**, *7*, 105023. [CrossRef]
78. Hamzaban, M.; Büyüksağiş, I.S.; Touranchehzadeh, A.; Manafi, M. The Effect of Heat Shocks and Freezing–Thawing Cycles on the Mechanical Properties of Natural Building Stones. *J. Mod. Mech. Eng. Technol.* **2021**, *8*, 76–100. [CrossRef]
79. Yang, Z.; Dou, L.; Liu, C.; Xu, M.; Lei, Z.; Yao, Y. Application of high-pressure water jet technology and the theory of rock burst control in roadway. *Int. J. Min. Sci. Technol.* **2016**, *26*, 929–935. [CrossRef]
80. Lu, Y.; Tang, J.; Ge, Z.L.; Xia, B.; Liu, Y. Hard rock drilling technique with abrasive water jet assistance. *Int. J. Rock Mech. Min. Sci.* **2013**, *60*, 47–56. [CrossRef]
81. Tripathi, R.; Srivastava, M.; Hloch, S.; Adamčíkc, P.; Chattopadhyayaa, S.; Das, A.K. Monitoring of acoustic emission during the disintegration of rock. *Procedia Eng.* **2016**, *149*, 481–488. [CrossRef]